Biogeosciences

Open Access

Interannual variation in summer N$_2$O concentration in the hypoxic region of the northern Gulf of Mexico, 1985–2007

I.-N. Kim[1], K. Lee[1], H. W. Bange[2], and A. M. Macdonald[3]

[1]School of Environmental Science and Engineering, POSTECH, Pohang 790-784, South Korea
[2]Marine Biogeochemie, GEOMAR Helmholtz-Zentrum für Ozeanforschung Kiel, 24105 Kiel, Germany
[3]WHOI, MS 21, 266 Woods Hold Rd., Woods Hole, MA 02543, USA

Correspondence to: K. Lee (ktl@postech.ac.kr)

Abstract. Microbial nitrous oxide (N$_2$O) production in the ocean is enhanced under low-oxygen (O$_2$) conditions. This is especially important in the context of increasing hypoxia (i.e., oceanic zones with extremely reduced O$_2$ concentrations). Here, we present a study on the interannual variation in summertime nitrous oxide (N$_2$O) concentrations in the bottom waters of the northern Gulf of Mexico (nGOM), which is well-known as the site of the second largest seasonally occurring hypoxic zone worldwide. To this end we developed a simple model that computes bottom-water N$_2$O concentrations with a tri-linear ΔN$_2$O$/$O$_2$ relationship based on water-column O$_2$ concentrations, derived from summer (July) Texas–Louisiana shelf-wide hydrographic data between 1985 and 2007. ΔN$_2$O (i.e., excess N$_2$O) was computed including nitrification and denitrification as the major microbial production and consumption pathways of N$_2$O. The mean modeled bottom-water N$_2$O concentration for July in the nGOM was 14.5 ± 2.3 nmol L^{-1} (min: 11.0 ± 4.5 nmol L^{-1} in 2000 and max: 20.6 ± 11.3 nmol L^{-1} in 2002). The mean bottom-water N$_2$O concentrations were significantly correlated with the areal extent of hypoxia in the nGOM. Our modeling analysis indicates that the nGOM is a persistent summer source of N$_2$O, and nitrification is dominating N$_2$O production in this region. Based on the ongoing increase in the areal extent of hypoxia in the nGOM, we conclude that N$_2$O production (and its subsequent emissions) from this environmentally stressed region will probably continue to increase into the future.

1 Introduction

Nitrous oxide (N$_2$O) has a lifetime of ~ 120 yr in the atmosphere, where it has two major effects: it contributes to both the greenhouse effect in the troposphere and the depletion of ozone in the stratosphere (IPCC, 2007; Ravishankara et al., 2009). The atmospheric N$_2$O concentration has increased rapidly since the 18th century, primarily because of anthropogenic activities (IPCC, 2007; Machida et al., 1995). The oceans are a major source of atmospheric N$_2$O, with oceanic emissions of N$_2$O accounting for approximately 20 % (4–7 Tg N yr^{-1}) of the total annual emissions (16–34 Tg N yr^{-1}) (Nevison et al., 1995; Seitzinger et al., 2000; Bange, 2006). Among identified oceanic sources, coastal oceans account for up to 60 % of the total oceanic N$_2$O emissions (Bange et al., 1996). The production of N$_2$O in coastal oceans is projected to increase worldwide (Bange, 2000; Naqvi et al., 2010), in proportion to the extent and intensity of eutrophication and hypoxia (Diaz and Rosenberg, 2008; Rabalais et al., 2009). The amount of N$_2$O produced during nitrification and denitrification, which are the major production processes of N$_2$O in the ocean, strongly depends on the prevailing oxygen (O$_2$) concentration. N$_2$O production is significantly enhanced under low O$_2$ concentrations (Codispoti, 2010). However, N$_2$O consumption occurs as O$_2$ concentrations decrease toward zero levels (e.g., O$_2 < 0.13$ mg L^{-1} (≈ 4 µM)) (Nevison et al., 2003, and references therein).

The northern Gulf of Mexico (nGOM) is widely considered to be a "dead zone" because of extreme eutrophication arising from nutrient loads that enter from adjacent rivers, including the Atchafalaya and Mississippi (Malakoff, 1998;

Justić et al., 2003; Turner and Rabalais, 2004). As a result, the area affected by hypoxia (defined here as an O$_2$ concentration $\leq 2\,\mathrm{mg\,L^{-1}}$ ($\approx 62.5\,\mu\mathrm{M}$)) increased to $\sim 20\,000\,\mathrm{km^2}$ during the past two decades (Rabalais et al., 2002) and has likely affected N$_2$O production (subsequent emissions to the atmosphere). Unfortunately, there are only a limited number of measurements of dissolved N$_2$O concentrations from the nGOM hypoxic zone available for September 2007, April, and July–August 2008 (see Visser, 2009, and Walker et al., 2010). According to Visser (2009) and Walker et al. (2010), the nGOM becomes a significant source of atmospheric N$_2$O during the summer with flux densities of $3.3–43.9\,\mu\mathrm{mol\,N_2O\,m^{-2}\,d^{-1}}$. At present, the summer nGOM N$_2$O emission rates ($0.2–2.3 \times 10^{-2}\,\mathrm{Tg\,N_2O\,yr^{-1}}$ extrapolated to an area of $\sim 3.24 \times 10^{10}\,\mathrm{m^2}$) are $<2\,\%$ of total N$_2$O emission rates from marine low-oxygen environments ($1.5–3.1\,\mathrm{Tg\,N_2O\,yr^{-1}}$, Naqvi et al. (2010) and references therein). However, the magnitudes of the summer nGOM N$_2$O fluxes are comparable to those associated with open-ocean hypoxic zones ($2.7–4.5\,\mu\mathrm{mol\,N_2O\,m^{-2}\,d^{-1}}$), enclosed anoxic basins ($1.6–5.2\,\mu\mathrm{mol\,N_2O\,m^{-2}\,d^{-1}}$), and naturally formed continental-margin hypoxic zones ($10–50\,\mu\mathrm{mol}$ $\mathrm{N_2O\,m^{-2}\,d^{-1}}$) (Naqvi et al., 2010, and references therein). Despite the fact that the nGOM has received much attention as a notorious "dead zone", it is not known how N$_2$O emissions from the nGOM have evolved throughout time. Addressing these unknowns will help to establish a modeling framework for the prediction of the future production and release of N$_2$O from the nGOM as well as from other comparable coastal areas throughout the globe. This is especially important in view of the fact that the number of hypoxic areas is increasing worldwide.

Using a simple model framed in terms of measured seawater O$_2$ levels and long-term summer hydrographic data collected from the nGOM, we estimate the evolution of bottom-water N$_2$O concentrations in Texas–Louisiana shelf regions for the month of July from 1985 to 2007.

2 Methods

2.1 Study area and data

The continental shelf area of the nGOM broadly extends seaward, and is shallower than $100\,\mathrm{m}$ depth (Fig. 1). The characteristics of nGOM seawater are primarily determined by mixing of Gulf of Mexico saltwater with freshwater discharged from the Atchafalaya and Mississippi rivers (Fig. 1). In our analysis, we used observations (temperature, salinity, dissolved O$_2$, nitrite + nitrate, phosphate and silicate) from Texas–Louisiana shelf-wide surveys regularly conducted in July (approximately 80 stations were occupied during each of the surveys). These July data for the period 1985–2007 (excluding the three years between 1988 and 1990) are available online: http://www.nodc.noaa.gov and http://www.

Fig. 1. The study area map showing the summer Texas–Louisiana shelf-wide cruise stations (red dots) during July 1985–2007 with the bathymetry contours (black dotted lines) in the northern Gulf of Mexico.

aoml.noaa.gov/ocd/necop/. The websites also provide information concerning the hydrographic cruises and the analytical methods used for nutrient analysis. Nutrients were measured at only two depths (near-surface and near-bottom). Our calculation of N$_2$O concentrations is based on the water samples collected near the shelf bottom.

2.2 A conceptual biogeochemical model for estimating N$_2$O production and consumption

In general, the tracer conservation equation at a fixed position is expressed as

$$\frac{\partial C}{\partial t} = \frac{\partial C}{\partial t_{\text{advection}}} + \frac{\partial C}{\partial t_{\text{diffusion}}} + J(C), \tag{1}$$

where C is tracer concentration, and $J(C)$ represents the net sources and sinks.

The tracer continuity equation for ΔN$_2$O ($=$ [N$_2$O]$_{\text{estimated}}$–[N$_2$O]$_{\text{equilibrium}}$) in the bottom layer associated with microbial processes (i.e., nitrification and denitrification by Bacteria and Archaea) is expressed as follows:

$$\Gamma(\Delta\mathrm{N_2O}) = J_{\text{nitrification}}(\Delta\mathrm{N_2O}) + J^{+}_{\text{low oxygen}}(\Delta\mathrm{N_2O}) \tag{2}$$
$$+ J^{-}_{\text{low oxygen}}(\Delta\mathrm{N_2O}),$$

where $J(\Delta\mathrm{N_2O})$ represents the function describing net production (i.e., source) minus consumption (i.e., sink) for each process. $J_{\text{nitrification}}(\Delta\mathrm{N_2O})$ denotes the source term for nitrification, $J^{+}_{\text{low oxygen}}(\Delta\mathrm{N_2O})$ the N$_2$O production during low O$_2$, and $J^{-}_{\text{low oxygen}}(\Delta\mathrm{N_2O})$ the N$_2$O consumption during
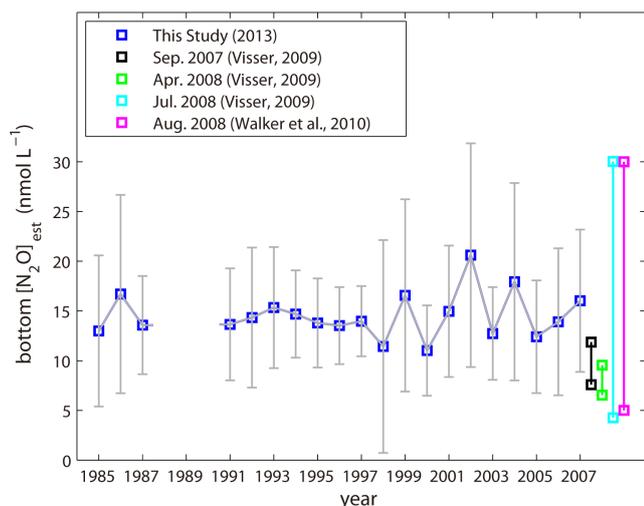
Fig. 2. Interannual variation of estimated bottom-water N$_2$O concentrations (blue square) in the nGOM during July 1985–2007. Measurements are included (black, green, cyan, and pink squares: September 2007, April 2008, July 2008, and August 2008, respectively).

low O$_2$ (Fig. S1). The operator Γ is the transport and time rate of change and is given as

$$\Gamma(C) = \frac{\partial C}{\partial t} + U \cdot \nabla C - \nabla \cdot (V \cdot \nabla C), \tag{3}$$

where C is any tracer concentration (here, it is ΔN$_2$O), ∇ denotes the gradient operator in the x, y, and z directions, U is the 3-dimensional velocity field, and V is the eddy diffusivity.

Under low-oxygen conditions, such as suboxic and anoxic conditions, anaerobic ammonium oxidation (anammox) and dissimilatory nitrate reduction to ammonium (DNRA) could be additional sources of N$_2$O (Naqvi et al., 2010). However, the pathways and yields of N$_2$O production during these two processes are poorly known. Furthermore, measurements of anammox and DNRA in the nGOM are in short supply (Dagg et al., 2007). As a result, we did not explicitly include the N$_2$O production by anammox and DNRA in our model. Instead, we assumed that the low oxygen terms ($J_{\text{low oxygen}}$) are determined by denitrification alone.

Since ΔN$_2$O is associated with microbial processes, we assume that transport by advection and diffusion is negligible, and, therefore, we drop the second and third terms on the right-hand side of Eq. (3). ΔN$_2$O is only determined by nitrification and denitrification. So, Eq. (2) is simplified to

$$\frac{\partial \Delta N_2 O}{\partial t} = J_{\text{nitrification}}(\Delta N_2 O) + J_{\text{low oxygen}}^+(\Delta N_2 O) + J_{\text{low oxygen}}^-(\Delta N_2 O) \tag{4}$$

Either a numerical or analytical approach can be used to solve the partial derivative Eq. (4). However, to date, exact $J(\Delta N_2 O)$ terms for the right-hand side are not known. Therefore, we assumed a tri-linear $\Delta N_2 O / O_2$ relationship

(Fig. S1). The use of a simple tri-linear $\Delta N_2 O / O_2$ relationship may increase the uncertainty of our modeled results, but can be taken as a simple best-guess approach. Using the empirically derived linear relationships, an analytical solution for $\Delta N_2 O$ may be derived as

$$\Delta N_2 O = \alpha \left(\frac{\text{nmol N}_2 O}{\mu\text{mol O}_2} \right) \cdot \text{AOU} + \beta \left(\frac{\text{nmol N}_2 O}{\mu\text{mol N}} \right) \\ \cdot \ \Delta N_{\text{deni}} - \gamma \left(\frac{\text{nmol N}_2 O}{\mu\text{mol N}} \right) \cdot \Delta N_{\text{deni}}, \tag{5}$$

where AOU is the apparent oxygen utilization – the difference between the measured O$_2$ concentration and the O$_2$ equilibration value, the coefficient of α indicates the relationship between ΔN$_2$O and AOU, and the coefficients of β and γ are the relationships between ΔN$_2$O and the amount of denitrification (ΔN$_{\text{deni}}$) that is the loss of nitrate (NO$_3^-$) as a consequence of denitrification. Finally, [N$_2$O]$_{\text{est}}$ can be estimated as

$$[N_2 O]_{\text{est}} = \Delta N_2 O + [N_2 O]_{\text{equilibrium}}^{(T, S)} \tag{6}$$

The values of these coefficients applicable to the nGOM are empirically determined to be 0.048, 0.83, and 0.83 for α, β, and γ, respectively. The rationale for choosing these values is described in Sect. 3.1. The procedures for estimating bottom-water N$_2$O concentrations in the nGOM are schematically presented in Fig. S2.

2.3 The O$_2$ criteria for determining nitrogen (N) processes that dominate N$_2$O production and consumption

We used Eq. (6) along with observations to estimate the N$_2$O concentrations in the near-bottom waters in the nGOM. The determination of which nitrogen processes (i.e., nitrification and denitrification) dominate N$_2$O production/consumption depends primarily on O$_2$ concentrations. Often hypoxia is defined as $0.14 < O_2 \leq 2\,\text{mg L}^{-1}$ ($\approx 62.5\,\mu$M), suboxia as $0 < O_2 \leq 0.14\,\text{mg L}^{-1}$ ($\approx 4.5\,\mu$M), and anoxia as $O_2 = 0\,\text{mg L}^{-1}$, based on O$_2$ levels (e.g., Naqvi et al., 2010). As little information is available on the O$_2$ threshold for N$_2$O production by denitrification, we deduced β and γ from the results of Farías et al. (2009) for our analysis. However, it should be kept in mind that these values were based on measurements from the eastern tropical South Pacific Ocean, and thus represent only a rough approximation.

In order to evaluate the O$_2$ dependence of our N$_2$O estimations, we considered two cases (Table 1). Case I characterizes the O$_2$ conditions as stated in Naqvi et al. (2010). Under oxic conditions, N$_2$O is produced by nitrification only, and thus the concentration is calculated as $\alpha \times$ AOU (Yoshinari, 1976; Cohen and Gordon, 1979; Oudot et al., 1990). Recently, Farías et al. (2009) showed net N$_2$O production around hypoxic O$_2$ levels in the eastern tropical South Pacific Ocean (see their Table 1). Under hypoxic conditions, during which nitrification and denitrification are both involved in N$_2$O

Table 1. Summary of O$_2$ criteria determining nitrogen (N) processes affecting N$_2$O production and consumption according to Cases I and II. Case II is given to examine the sensitivity on the threshold O$_2$ values for N$_2$O production/consumption by denitrification.

Case I			
O$_2$ levels (mg L^{-1})	Conditions	N process	N$_2$O estimation
$2 < O_2$	oxic	Nitrification	$\alpha \times$ AOU
$0.14 \leq O_2 \leq 2$	hypoxic	Nitrification + denitrification (+)	$\alpha \times$ AOU $+ \beta \times \Delta$N$_{deni}$
$0 \leq O_2 < 0.14$	suboxic–anoxic	Nitrification + denitrification (−)	$\alpha \times$ AOU $- \gamma \times \Delta$N$_{deni}$
Case II			
O$_2$ levels (mg L^{-1})	Conditions	N process	N$_2$O estimation
$2 < O_2$	oxic	Nitrification	$\alpha \times$ AOU
$0.07 \leq O_2 \leq 2$	suboxic–hypoxic	Nitrification + denitrification (+)	$\alpha \times$ AOU $+ \beta \times \Delta$N$_{deni}$
$0 \leq O_2 < 0.07$	suboxic–anoxic	Nitrification + denitrification (−)	$\alpha \times$ AOU $- \gamma \times \Delta$N$_{deni}$

+(−): N$_2$O production(consumption) by denitrification.

production (Naqvi et al., 1998; Nevison et al., 2003), N$_2$O concentrations were calculated as $\alpha \times$ AOU $+ \beta \times \Delta$N$_{deni}$. It has been reported that N$_2$O consumption occurs at O$_2$ $< \sim 4\,\mu$M (≈ 0.13 mg L^{-1}) (Nevison et al., 2003, and references therein). Under such suboxic–anoxic conditions, denitrification consumes N$_2$O (Cohen and Gordon, 1978; Elkins et al., 1978; Yamagishi et al., 2007), and nitrification produces N$_2$O via nitrite reduction (nitrifier denitrification: NH$_4^+ \rightarrow$ NO$_2^- \rightarrow$ N$_2$O) (Poth and Focht, 1985; Wrage et al., 2001). Therefore, under these conditions N$_2$O concentrations were calculated as $\alpha \times$ AOU $- \gamma \times \Delta$N$_{deni}$.

For Case II the same approach was adopted as for Case I, and different O$_2$ thresholds were applied: (1) oxic conditions defined as O$_2 > 2$ mg L^{-1} ($\alpha \times$ AOU), (2) hypoxic–suboxic conditions defined as $0.07 \leq O_2 \leq 2$ mg L^{-1} ($\alpha \times$ AOU $+ \beta \times \Delta$N$_{deni}$), and (3) suboxic–anoxic conditions defined as $0 \leq O_2 < 0.07$ mg L^{-1} ($\approx 2.2\,\mu$M) ($\alpha \times$ AOU $- \gamma \times \Delta$N$_{deni}$).

2.4 Information of denitrification (ΔN$_{deni}$) estimated in the nGOM

The ΔN$_{deni}$ term plays a crucial role in the estimation of bottom-water N$_2$O concentrations (Eq. 5). The ΔN$_{deni}$ was estimated using the extended optimum multi-parameter (eOMP) analysis by Kim and Min (2013) with the same summer Texas–Louisiana shelf-wide hydrographic data sets used here. The eOMP analysis is a useful way to quantify physical mixing and biogeochemical processes simultaneously (Karstensen and Tomczak, 1998; Hupe and Karstensen, 2000). It is an inverse method based on an over-determined linear system, and its basic structure is given as

$$\mathbf{A} \cdot \boldsymbol{x} - \boldsymbol{d} = \boldsymbol{R}, \tag{7}$$

where the matrix $\mathbf{A}$ is composed of the physicochemical characteristics of end-members that participate in physical mixing in the study area, and the Redfield ratios that represent biogeochemical processes. The vector $\boldsymbol{x}$ consists of the unknowns including mixing ratios

among different pre-defined water masses, the amount of remineralized phosphate (ΔP$_{remi}$), and denitrification (ΔN$_{deni}$), whereas the vector $\boldsymbol{d}$ contains the observed values, and the vector $\boldsymbol{R}$ represents the constraint residuals. For the characteristics of pre-defined water masses, Kim and Min (2013) defined four different water masses: low temperature and high salinity waters as Subtropical Underwater (SUW) ($18.6 \pm 0.3\,°$C and 36.7 ± 0.1), high temperature and high salinity waters as Texas–Louisiana Coastal Water (TLCW) ($29.6 \pm 0.4\,°$C and 35.3 ± 0.2), and two freshwaters as Atchafalaya Discharge Water (ADW) ($31.1 \pm 0.6\,°$C and 0) and Mississippi Discharge Water (MDW) ($29.4 \pm 1.0\,°$C and 0). They considered four different Redfield ratio cases ($r_{\text{Si:N:P:}-\text{O2}=15:16:1:138}$, $r_{\text{Si:N:P:}-\text{O2}=15:16:1:150}$, $r_{\text{Si:N:P:}-\text{O2}=16:11:1:138}$, and $r_{\text{Si:N:P:}-\text{O2}=16:11:1:150}$), and then reported mean values of biogeochemical changes (i.e., ΔP$_{remi}$ and ΔN$_{deni}$) averaged from four different results. The results of this eOMP analysis produced residuals for the mass conservation equations $< \sim 2\,\%$. Further details can be found in Kim and Min (2013). Here, we used the results of denitrification (ΔN$_{deni}$) estimated from the eOMP analysis by Kim and Min (2013) for this study.

3 Results and discussion

3.1 Determination of the coefficients α, β and γ in the conceptual model

The coefficients of α, β, and γ in Eq. (5) are known to vary as a result of mixing of water masses, changes in the rates of nitrification/denitrification, and variations in the chemical composition of organic matter produced in situ (Cohen and Gordon, 1978; Elkins, 1978; Nevison et al., 2003). This, in turn, implies that the applicability of the three coefficients for estimating N$_2$O concentrations will vary on a regional scale (Suntharalingam et al., 2000). Walker et al. (2010) measured N$_2$O in the waters of the nGOM between August 2 and 7,
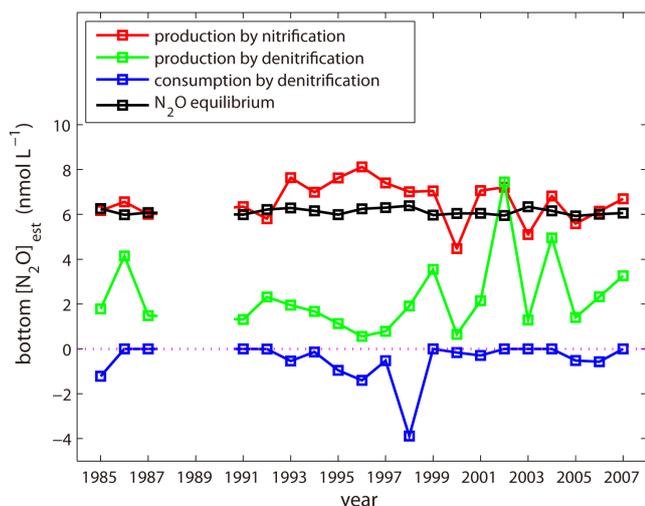
Fig. 3. The individual contributions of nitrification (red squares, production), denitrification (green squares, production), denitrification (blue squares, consumption), and N$_2$O equilibrium (black squares) to the bottom-water N$_2$O concentrations in the nGOM from July 1985 to 2007.
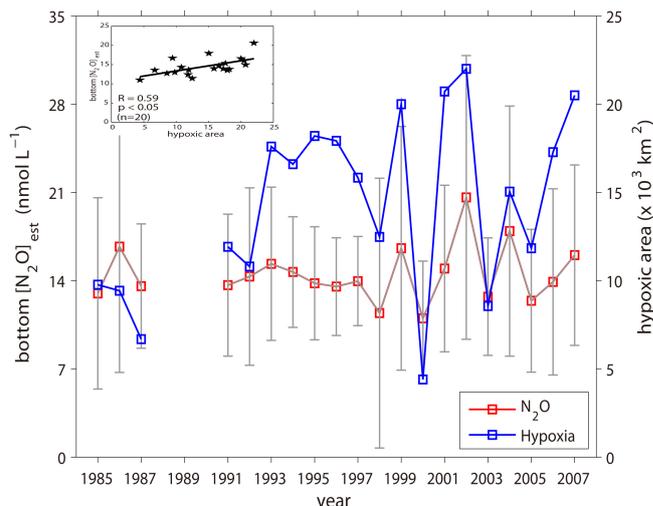

Fig. 4. Interannual variations in summer (July) bottom-water N$_2$O concentration (nmol L^{-1}, red squares) and the areal extent of hypoxia (km^2, blue squares). The estimated bottom-water N$_2$O concentrations were significantly correlated with the areal extent of hypoxia ($R = 0.59$; $p < 0.05$ with $n = 20$). Data concerning the areal extent of hypoxia are available at http://www.gulfhypoxia. net/Research/Shelfwide%20Cruises/ (data source: N. N. Rabalais, Louisiana Universities Marine Consortium, R. E. Turner, Louisiana State University).

2008, when a tropical storm (i.e., Edouard) passed over the nGOM on 4 August. This gave Walker et al. (2010) the opportunity to compare pre-storm with post-storm N$_2$O production. They reported enhanced N$_2$O post-storm production, resulting from a reoxygenation of the water column after the storm. The estimated α values for pre-storm and post-storm conditions based on ΔN$_2$O / AOU relationships were 0.048 and 0.096, respectively (see their Fig. 4). Since the factors known to influence α in the nGOM are probably at their most extreme immediately following the storm event, it is likely that $\alpha = 0.096$ is an upper limit. The data sets used for the present analysis were little influenced by storm/hurricane events (Table S1), which enhance N$_2$O production only for very short periods. Therefore, we assumed that $\alpha = 0.048$ is a representative summertime nGOM coefficient for N$_2$O production by nitrification.

We assigned a value 0.83 to the coefficient β for the nGOM. This value was derived from an incubation experiment in the eastern tropical South Pacific Ocean (ETSP) (see Fig. 4 of Farías et al., 2009). We adopted this estimate in our modeling because no comparable data from the nGOM are available. During the denitrification process N$_2$O is also consumed. The amount consumed is quantitatively related to the O$_2$ level. Farías et al. (2009) varied the ratio of N$_2$O production vs. consumption from 0.36 to 6.55 according to oxygen levels in the ETSP (see Fig. 5 of Farías et al., 2009). It is determined that the ratio under suboxic–anoxic conditions is 1 on average. Therefore, we assumed $\gamma \approx \beta$ for the purpose of our modeling exercise. The choice of values for the coefficients β and γ is less critical than the choice of α, because

N$_2$O production associated with β and γ typically represents less than $\sim 15\%$ of the total production (Fig. 3).

3.2 Sensitivity, uncertainty, and caveat

We assigned 0.048, 0.83, and 0.83 for α, β, and γ, respectively, to estimate bottom-water N$_2$O concentrations using the empirical relationship presented in Sect. 3.1. To investigate the validity of chosen values of α, β, and γ, we used a Monte Carlo technique generating random numbers for individual α, β, and γ values within expected ranges looking for those coefficients that produced estimated bottom-water N$_2$O concentrations within the observed range. The value of α ranges from 0.048 to 0.31 in various ocean environments, including the nGOM (Suntharalingam and Sarmiento, 2000, and references therein). For our model simulation we generated random numbers for α between 0 and 0.31. We deduced β and γ from the results of Farías et al. (2009), since information on β and γ from other oceanic regions is lacking. We, therefore, have increased the possible range in these values that generated random numbers for β and γ between 0 and 2.5. In the nGOM, Visser (2009) and Walker et al. (2010) directly measured water-column N$_2$O concentrations during the summer of 2008, and reported that bottom-water N$_2$O concentrations ranged from 4.25 to 30.02 nmol L^{-1} (July) and from 5 to 30 nmol L^{-1} (August). Bottom-water N$_2$O concentrations were similar in both months, so we used the median of measured values (17–18 nmol L^{-1}) as the
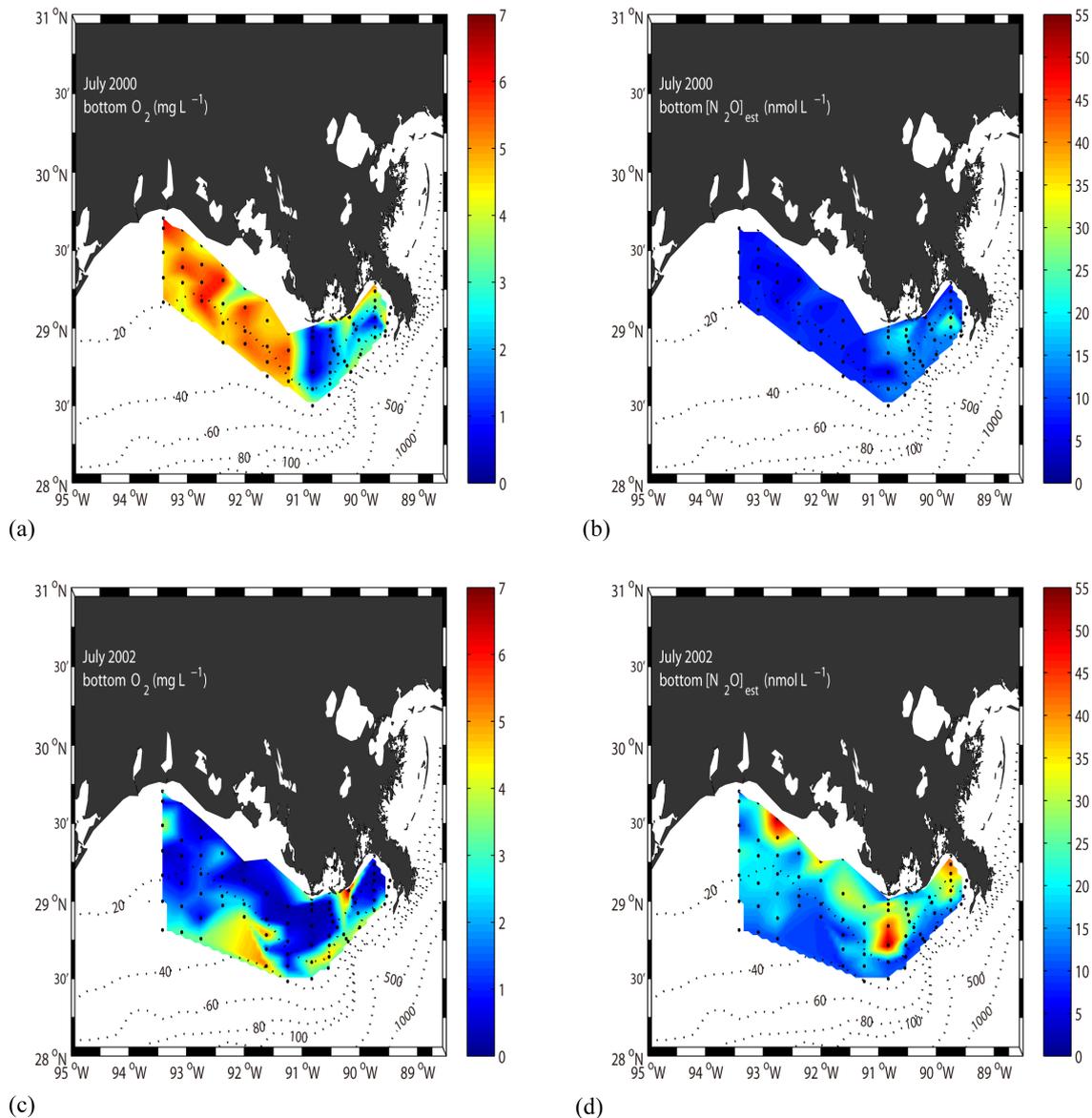
Fig. 5. Distributions of observed bottom-water O_2 and estimated bottom-water N_2O concentrations in July 2000 and 2002, representing min. and max. hypoxic areal extent during the study period, respectively. **(a)** and **(b)** indicate bottom-water O_2 and N_2O spatial distributions in July 2000. **(c)** and **(d)** denote bottom-water O_2 and N_2O spatial distributions in July 2002.

acceptable zone, and then applied the random α, β, and γ values to the data sets to estimate N_2O concentrations. When the mean N_2O concentration reproduced by random α, β, and γ values fell in the acceptable range (i.e., $17 <$ mean $[N_2O] < 18$), they were saved and averaged. We generated a thousand of random numbers for individual α, β, and γ for each simulation, and performed 10 simulations (Fig. S3). The resulting α, β, and γ coefficients averaged over all the simulations were 0.051 ± 0.003, 1.27 ± 0.15, 1.16 ± 0.16, respectively. The $\alpha = 0.048$ obtained from the empirical relationship compared well with the simulated $\alpha = 0.051 \pm 0.003$. The $\beta = 0.83$ and $\gamma = 0.83$ are somewhat lower than the

simulated $\beta = 1.27 \pm 0.15$ and $\gamma = 1.16 \pm 0.16$. The change of N_2O concentrations according as α, β, and γ individually change with 0.01 interval was ~ 1.3, ~ 0.03, and ~ 0.001 nmol L^{-1}, respectively.

To examine the sensitivity to the threshold O_2 values for N_2O production/consumption by denitrification (Table 1), Case I estimates were compared with Case II. On average, the N_2O concentrations estimated for Case I were ~ 0.9 nmol L^{-1} lower than those by Case II (Fig. S4). Also, both temporal trends were similar. Thus, the results of Case I are primarily used for our study.

Kim and Min (2013) defined four different water masses (i.e., SUW: Subtropical Underwater, TLCW: Texas–Louisiana Coastal Water, ADW: Atchafalaya Discharge Water, and MDW: Mississippi Discharge Water) for the eOMP analysis in the study area. Unlike the others, SUW is a foreign water mass that only occasionally intrudes into the study area depending on eddy development/circulation patterns. Although it is difficult to estimate preformed N$_2$O concentrations for each water mass from this analysis, because SUW locally occupies the bottom layer and is derived from outside the study area, it is possible to approximate the amount of N$_2$O advected by SUW using a plot of the estimated bottom-water N$_2$O concentrations vs. the mixing ratios of SUW (Fig. S5). Higher mixing ratios of SUW imply that the water properties are close to those of the source water mass, and by using a constraint on SUW mixing ratios of > 90 %, the N$_2$O concentrations produced through advection of SUW into the nGOM region is estimated to be 13.3 ± 2.5 nmol L^{-1}, which is the mean value averaged from the N$_2$O concentrations for SUW mixing rations > 90 % (Fig. S5). This estimate is close to the overall N$_2$O mean concentration of 14.5 ± 2.3 nmol L^{-1} for the nGOM. However, SUW is only locally found in the study area ($\sim$ 89.5–92° W and 28.5–29.0° N deeper than $\sim$ 40 m), and its occurrence in the nGOM bottom waters has been decreasing since $\sim$ 1998 (Kim and Min, 2013). Therefore, the overall effect of N$_2$O advected by SUW seems to be small.

Our model cannot directly account for possible N$_2$O sediment fluxes, as ΔN_{deni} signals estimated by Kim and Min (2013) in the bottom waters cannot be distinguished from those derived from sediments. Therefore, we assumed that the estimated N$_2$O concentrations from this study were resulting from bottom-water and sedimentary processes combined (i.e., benthic coupling processes). In the following section, we quantify the contribution by denitrification to the total N$_2$O concentration.

Here we estimated bottom-water N$_2$O concentrations using the tri-linear relationships between O$_2$ and ΔN_2O. This approach provided a representation of interannual N$_2$O variations in the nGOM. However, it has several limitations: (i) the lack of α variability in the nGOM (i.e., interannual and seasonal), (ii) little information on β and γ for the nGOM, and (iii) an unknown shape of the $\Delta N_2O/O_2$ relationship. Due to such limitations, we remind the readers that our estimates are based on empirically derived relationships and are valid only in the nGOM and only during the summer. In order to estimate N$_2$O concentrations accurately using modeling approaches, integrated information on α, β, and γ based on direct measurements will be needed to establish a non-linear equation in the future.

3.3 Mechanisms of N$_2$O production and consumption in the nGOM

For the period 1985–2007, the July mean N$_2$O concentration in near-bottom waters of the nGOM is estimated to be 14.5 ± 2.3 nmol L^{-1} (min: 11.0 ± 4.5 nmol L^{-1} in July 2000, max: 20.6 ± 11.3 nmol L^{-1} in July 2002), with large interannual variability (Table 2). The range of bottom-water N$_2$O measurements during the summer (July–August) of 2008 was from 4.5 to 30.0 nmol L^{-1} (Visser, 2009; Walker et al., 2010), and during the spring/fall (September 2007 and April 2008) from 6.5 to 12.0 nmol L^{-1} (Visser, 2009) (Fig. 2). Thus, we conclude that our estimates are in good agreement with the measurements. Comparing the nGOM estimates with those observed in other hypoxic coasts (Table 2b of Naqvi et al., 2010, and references therein), it can be seen that maximum subsurface N$_2$O concentrations in the anthropogenically produced coastal hypoxic systems have a broad range from 9.8 nmol L^{-1} in the Chesapeake Bay to 62.6 nmol L^{-1} in the Changjiang Estuary, to 139 nmol L^{-1} in the Tokyo Bay. Estimates from the nGOM ($\sim$ 30 nmol L^{-1}) lie in the middle of this range according to Naqvi et al. (2010). The maximum N$_2$O concentration estimated in our analysis was $\sim$ 52 nmol L^{-1} (Table 2).

The mean bottom-water N$_2$O concentration for July 1998 (11.4 ± 10.7 nmol L^{-1}) was relatively low for the study period, but the areal extent of hypoxia in 1998 was relatively large (> 12 000 km^2) (Fig. 4). This was caused by the fact that the estimated N$_2$O concentrations were significantly influenced by N$_2$O consumption in July 1998 (Fig. 3). In July 2000, the mean bottom-water N$_2$O concentration (11.0 ± 4.5 nmol L^{-1}) was lower compared to other years. However, in contrast to 1998, the areal extent of the hypoxia in 2000 was smaller ($\sim$ 4400 km^2) (Figs. 4 and 5). The following scenario may explain the lower N$_2$O concentration and smaller areal extent of hypoxia found in July 2000. The total freshwater discharge from the Mississippi and Atchafalaya rivers in the period January–July 2000 was less than in the same period in other years (Fig. S6), resulting in decreased production of organic matter through biological productivity (Walker and Rabalais, 2006). This feature is consistent with the interannual variation of mixing ratios of ADW and MDW (Fig. S7). Consequently, the oxidation of organic matter was probably decreased, and the net effect was a reduction in the areal extent of hypoxia in July 2000. Another contrasting example is evident for July 2002. The mean bottom-water N$_2$O concentration was highest (20.6 ± 11.3 nmol L^{-1}), and the size of the hypoxic zone was largest ($\sim$ 22 000 km^2) (Fig. 4). The N$_2$O production by denitrification was also highest in July 2002, and its contribution to the overall N$_2$O production was also significant (Fig. 3). These conditions probably resulted in July 2002 having the highest N$_2$O concentration (Fig. 5). Overall, interannual variation in the estimated bottom-water N$_2$O

Table 2. Mean bottom-water N$_2$O concentrations (nmol L^{-1}) during the study period estimated from Eq. (6) using $\alpha = 0.048$, $\beta = 0.83$, and $\gamma = 0.83$. The mean is calculated as $[N_2O]_{est}^{mean} = \frac{\sum_{i=1}^{n} [N_2O]_{est}^{i}}{n}$, where i is the estimate at one station, and n is the number of total estimates. Standard deviations ($\pm$) are calculated as $\sqrt{\frac{\sum_{i=1}^{n} ([N_2O]_{est}^{i} - [N_2O]_{est}^{mean})^2}{n}}$.

Year (for July)	$[N_2O]_{est}^{mean}$	maximum	remark
1985	13.0 ± 7.6	35.9	
1986	16.7 ± 10.0	52.4	
1987	13.6 ± 4.9	32.9	
1988	ND	ND	
1989	ND	ND	
1990	ND	ND	
1991	13.7 ± 5.6	38.4	
1992	14.3 ± 7.0	42.7	
1993	15.4 ± 6.1	31.7	
1994	14.7 ± 4.4	30.8	Visser (2009)
1995	13.8 ± 4.5	32.0	Sep 2007: 7.59–11.87 (mean: 9.95 ± 1.07)
1996	13.5 ± 3.9	22.5	April 2008: 6.53–9.54 (mean: 7.10 ± 0.70)
1997	14.0 ± 3.5	21.3	July 2008: 4.25–30.02 (mean: 11.00 ± 6.95)
1998	11.4 ± 10.7	31.8	
1999	16.6 ± 9.7	51.5	
2000	11.0 ± 4.5	29.1	Walker et al. (2010)
2001	15.0 ± 6.6	34.4	August 2008: 5–30 (pre-storm)
2002	20.6 ± 11.3	54.9	7–47 (post-storm)
2003	12.7 ± 4.7	27.6	
2004	17.9 ± 9.9	51.9	
2005	12.4 ± 5.7	23.3	
2006	13.9 ± 7.4	42.9	
2007	16.0 ± 7.2	42.6	

ND: not determined.

concentrations is significantly correlated with the areal extent of hypoxia ($R = 0.59$; $p < 0.05$; Fig. 4).

To identify the primary mechanism(s) of N$_2$O production in the nGOM, we estimate the contribution to N$_2$O concentration of each mechanism: production by nitrification and denitrification, consumption by denitrification, and N$_2$O equilibrium (Fig. 3). Our result indicates that $\sim 44\%$ of the total N$_2$O is produced by nitrification, and $\sim 14\%$ is produced by denitrification. The result also indicates that, with reasonable parameters for denitrification, the N$_2$O sink is small compared to the sources, and represents only a small contribution (approximately 1%) to the total N$_2$O concentration. The results of Visser (2009) showed that N$_2$O consumption can occur in the sediments and reported that the contribution of N$_2$O released from the sediments was negligible in the nGOM. Together, these results imply that water-column processes may be the dominant control for N$_2$O production in the nGOM. The remainder ($\sim 41\%$) is covered by N$_2$O equilibrium. Our study indicates that the nitrification is the major process responsible for the biological production of N$_2$O in the nGOM. This is also supported by the findings that the N$_2$O production by nitrification is significantly cor-

related with the areal extent of hypoxia (Fig. S8). Moreover, the total N$_2$O production by nitrification and denitrification shows a significant correlation with the amount of remineralized carbon as estimated by Kim and Min (2013) (Fig. S9).

Based on the significance of the correlation between the estimated bottom-water N$_2$O concentrations and the areal extent of hypoxia (Fig. 4), it is expected that the strength of the nGOM as a source of N$_2$O will increase into the future if the expansion of the hypoxic region in the nGOM continues. This is in line with the suggestions by Bange (2000), Naqvi et al. (2000), and Codispoti (2010).

4 Conclusions

The nGOM is receiving ever-increasing loads of nutrients through rivers from anthropogenic activities, and this has led to more intense and widespread hypoxic conditions (Rabalais et al., 2009; Bianchi et al., 2010). As the areal extent of nGOM hypoxia continues to expand, it is expected that N$_2$O production and its subsequent emissions to the atmosphere will be enhanced. In particular, it is expected that this study area will likely be more vulnerable to human-induced events

in the future. For these reasons, we need to improve our understanding of N_2O cycles in the nGOM. However, this investigation, as well as previous studies, has been severely limited by a distinct lack of information on the ΔN_2O coefficients (i.e., α, β, and γ). In particular, knowledge of interannual and seasonal variability in these terms would provide a fundamental step forward in our understanding of the nGOM N_2O cycles. Further, an increased number of direct N_2O measurements could improve our knowledge of the $\Delta N_2O / O_2$ relationship allowing an improvement in our modeling approach through a reduction in uncertainties. Our model results indicate that nitrification is the primary process responsible for the microbial N_2O production in the nGOM, implying that N_2O production is mainly controlled by water-column processes. This result suggests that future observational surveys in both the nGOM and perhaps also other coastal oceans can concentrate resources on the water column in an effort to improve the resolution of available time series.

Supplementary material related to this article is available online at http://www.biogeosciences.net/10/6783/2013/bg-10-6783-2013-supplement.pdf.

References

Bange, H. W.: It's not a gas, Nature, 408, 301–302, 2000.

Bange, H. W.: New directions: The importance of oceanic nitrous oxide emissions, Atmos. Environ., 40, 198–199, 2006.

Bange, H. W., Rapsomanikis, S., and Andreae, M. O.: Nitrous oxide in coastal waters, Global Biogeochem. Cy., 10, 197–207, 1996.

Bianchi, T. S., DiMarco, S. F., Cowan Jr., J. H., Hetland, R. D., Chapman, P., Day, J. W., and Allison, M. A.: The science of hypoxia in the northern Gulf of Mexico: A review, Sci. Total, Environ., 408, 1471–1484, 2010.

Codispoti, L. A.: Interesting times for marine N_2O, Science, 327, 1339–1340, 2010.

Cohen, Y. and Gordon, L. I.: Nitrous oxide in the oxygen minimum of the eastern tropical North Pacific: evidence for its consumption during denitrification and possible mechanisms for its production, Deep-Sea Res., 25, 509–524, 1978.

Cohen, Y. and Gordon, L. I.: Nitrous oxide production in the ocean, J. Geophys. Res., 84, 347–353, 1979.

Diaz, R. J. and Rosenberg, R.: Spreading dead zones and consequences for marine ecosystems, Science, 321, 926–929, 2008.

Elkins, J. W., Wofsy, S. C., McElroy, M. B., Kolb, C. E., and Kaplan W. A.: Aquatic sources and sinks for nitrous oxide, Nature, 275, 602–606, 1978.

Farías, L., Castro-González, M., Cornejo, M., Charpentier, J., and Faúndez, J.: Denitrification and nitrous oxide cycling within the upper oxycline of the eastern tropical South Pacific oxygen minimum zone, Limnol. Oceanogr., 54, 132–144, 2009.

Hupe, A. and Karstensen, J.: Redfield stoichiometry in Arabian Sea subsurface waters, Global Biogeochem. Cy., 14, 357–372, 2000.

IPCC: Climate Change 2007: The Physical Science Basis. Contribution of Working Group I to the Fourth Assessment Report of the Intergovermental Pannel on Climate Change, Cambridge University Press, Cambridge, UK and New York, NY, USA, 2007.

Justić, D., Turner, R. E., and Rabalais, N. N.: Climatic influences on riverine nitrate flux: Implications for coastal marine eutrophication and hypoxia, Estuaries, 26, 1–11, 2003.

Kim, I.-N. and Min, D.-H.: Temporal variation of summertime denitrification rates in the Texas-Louisiana inner shelf region in the Gulf of Mexico: A modeling approach using the extended OMP analysis, Cont. Shelf Res., 66, 49–57, 2013.

Machida, T., Nakazawa, T., Fujii, Y., Aoki, S., and Watanabe, O.: Increase in the atmospheric nitrous oxide concentration during the last 250 years, Geophys. Res. Lett., 22, 2921–2924, 1995.

Malakoff, D.: Death by suffocation in the Gulf of Mexico, Science, 281, 190–192, 1998.

Naqvi, S. W. A., Yoshinari, T., Jayakumar, D. A., Altabet, M. A., Narvekar, P. V., Devol, A. H., Brandes, J. A., and Codispoti, L. A.: Budgetary and biogeochemical implications of N_2O isotope signatures in the Arabian Sea, Nature, 394, 462–464, 1998.

Naqvi, S. W. A., Jayakumar, D. A., Narvekar, P. V., Naik, H., Sarma, V. V. S. S., D'Souza, W., Joseph, S., and George, M. D.: Increased marine production of N_2O due to intensifying anoxia on the Indian continental shelf, Nature, 408, 346–349, 2000.

Naqvi, S. W. A., Bange, H. W., Farías, L., Monteiro, P. M. S., Scranton, M. I., and Zhang, J.: Marine hypoxia/anoxia as a source of CH_4 and N_2O, Biogeosciences, 7, 2159–2190, doi:10.5194/bg-7-2159-2010, 2010.

Nevison, C. D., Weiss, R. F., and Erickson III, D. J.: Global oceanic emissions of nitrous oxide, J. Geophys. Res., 100, 15809–15820, 1995.

Nevison, C., Butler, J. H., and Elkins, J. W.: Global distribution of N_2O and the ΔN_2O-AOU yield in the subsurface ocean. Global Biogeochem. Cy., 17, 1119, doi:10.1029/2003GB002068, 2003.

Oudot, C., Andrie, C., and Montel, Y.: Nitrous oxide production in the tropical Atlantic Ocean, Deep-Sea Res., 37, 183–202, 1990.

Poth, M. and Focht, D. D.: [15]N kinetic analysis of N_2O production by Nitrosomonas europaea: an examination of nitrifier denitrification, Appl. Environ. Microbiol., 49, 1134–1141, 1985.

Rabalais, N. N., Turner, R. E., and Scavia, D.: Beyond science into policy: Gulf of Mexico hypoxia and the Mississippi River, BioSci., 52, 129–142, 2002.

Rabalais, N. N., Turner, R. E., Díaz, R. J., and Justić, D.: Global change and eutrophication of coastal waters, ICES J. Mar. Sci., 66, 1528–1537, 2009.

Ravishankara, A. R., Daniel, J. S., and Portmann, R. W.: Nitrous Oxide (N$_2$O): The dominant ozone-depleting substance emitted in the 21st Century, Science, 326, 123–125, 2009.

Seitzinger, S. P., Kroeze, C., and Styles, R. V.: Global distribution of N$_2$O emissions from aquatic systems: natural emissions and anthropogenic effects, Chemosphere-Global Change Sci., 2, 267–279, 2000.

Suntharalingam, P. and Sarmiento, J. L.: Factors governing the oceanic nitrous oxide distribution: Simulations with an ocean general circulation model, Global Biogeochem. Cy., 14, 429–454, 2000.

Suntharalingam, P., Sarmiento, J. L., and Toggweiler, J. R.: Global significance of nitrous-oxide production and transport from oceanic low-oxygen zones: A modeling study, Global Biogeochem. Cy., 14, 1353–1370, 2000.

Turner, R. E. and Rabalais, N. N.: Suspended sediment, C, N, P, and Si yields from the Mississippi River basin, Hydrobiol., 511, 79–89, 2004.

Visser, L. A.: Nitrous oxide production in the Gulf of Mexico hypoxic zone, M. S. thesis, Dep. of Oceanogr., Texas A&M Univ., College Station, Texas, USA, 2009.

Walker, N. D. and Rabalais, N. N.: Relationships among satellite chlorophyll a, river inputs, and hypoxia on the Louisiana continental shelf, Gulf of Mexico, Estuaries Coasts, 29, 1081–1093, 2006.

Walker, J. T., Stow, C. A., and Geron, C.: Nitrous oxide emissions from the Gulf of Mexico hypoxic zone. Environ. Sci. Technol., 44, 1617–1623, 2010.

Wrage, N., Velthof, G. L., van Beusichem, M. L., and Oenema, O.: Role of nitrifier denitrification in the production of nitrous oxide, Soil Biol. Biochem., 33, 1723–1732, 2001.

Yamagishi, H., Westley, M. B., Popp, B. N., Toyoda, S., Yoshida, N., Watanabe, S., Koba, K., and Yamanaka, Y.: Role of nitrification and denitrification on the nitrous oxide cycle in the eastern tropical North Pacific and Gulf of California, J. Geophys. Res., 112, G02015, doi:10.1029/2006JG000227, 2007.

Yoshinari, T.: Nitrous oxide in the sea, Mar. Chem., 4, 189–202, 1976.